Applied Mathematical Sciences, Vol. 8, 2014, no. 140, 6951 - 6961
HIKARI Ltd, www.m-hikari.com
http://dx.doi.org/10.12988/ams.2014.48616

Psychovisual Threshold on Large Tchebichef Moment for Image Compression

Nur Azman Abu

Faculty of Information and Communication Technology
Universiti Teknikal Malaysia Melaka, Melaka 76100, Malaysia

Ferda Ernawan

Faculty of Information and Communication Technology
Universiti Teknikal Malaysia Melaka, Melaka 76100, Malaysia
and
Faculty of Computer Science, Universitas Dian Nuswantoro
Semarang 50131, Indonesia

Abstract

JPEG standard transforms an 8×8 image pixel into a frequency domain. The discontinuities of the intensity image between adjacent image blocks cause the visual artifacts due to inter-block correlations in image reconstruction. The blocking artifacts appear by the pixel intensity value discontinuities which occur along block boundaries. This research proposes the psychovisual threshold on large Tchebichef moment to minimize the blocking artifacts. The psychovisual threshold is practically the best measure for the optimal amount of frequency image signals in the image coding. The psychovisual threshold is a basic element prior to generating quantization tables in image compression. The psychovisual threshold on the large Tchebichef moments has given significant improvements in the quality of image output. The experimental results show that the smooth psychovisual threshold on the large discrete Tchebichef moment produces high quality image output and largely free of any visual artifacts.

Keywords: TMT Quantization, Psychovisual Threshold, Tchebichef Moment Transform, Image Compression

1 Introduction

The JPEG image compression implements a basic 8×8 block transform coding. The block transform coding suffers noticeable quality image degradations near boundary blocks causes blocking artifact [1]. The most noticeable degradations on the block transform coding are often visually observable at high compression ratios [2]. Since the 8×8 blocks of image pixels are encoded separately, the correlation among spatially adjacent blocks provides boundary blocks when the image is reconstructed [3]. The block-size on the transform coding gives a significant effect to the quality of image compression. This experiment mainly focuses the block-size of the discrete transform and an optimal quantization values assigned to the frequency image signals. Previously, a psychovisual threshold has been investigated on 8×8 Tchebichef image compression [4]. In this paper, the same concept of the psychovisual threshold on 8×8 Tchebichef moments is adopted to develop the psychovisual threshold on 256×256 Tchebichef moment in image compression. The smooth psychovisual threshold is an input to generating 256×256 Tchebichef quantization table for lossy image compression. In this paper, the large 256×256 Tchebichef Moment Transform (TMT) has been chosen here since TMT has not been practically explored on large image compression. TMT has been widely used in various image processing applications. For examples, they are used in image watermarking [5], image compression [6-10] and image dithering [11].

2 Orthonormal Tchebichef Moment Transform

In this experiment, the contribution of the discrete orthonormal Tchebichef moment to the image quality shall be explored for image compression. The discrete orthonormal Tchebichef moment provides a compact support on the large image block [12]. On large image block, an accumulation of numerical error gets reduced down due to larger moment order. The discrete orthonormal Tchebichef transform has energy compactness properties on the large image block. For a given set $\{t_n(x)\}$ of input value (image intensity values) of size N=256, the forward orthonormal Tchebichef transform of order $m + n$ is given as follows [12]:

$$T_{mn} = \sum_{x=0}^{M-1}\sum_{y=0}^{N-1} \frac{t_m(x)}{\rho(m,M)} f(x,y) \frac{t_n(y)}{\rho(n,N)} = \sum_{x=0}^{M-1}\sum_{y=0}^{N-1} k_m(x) f(x,y) k_n(y)$$

For m = 0, 1, 2, ..., M-1 and $f(x,y)$ denotes the intensity value of an image at the pixel position x and y. The $t_n(x)$ is defined using the following recursive relation:

$$t_n(x) = \alpha_1 x t_{n-1}(x) + \alpha_2 t_{n-1}(x) + \alpha_3 t_{n-2}(x),$$

for n = 2, 3, ..., N-1 and x = 0, 1, ..., N-1. Where

$$\alpha_1 = \frac{2}{n}\sqrt{\frac{4n^2-1}{N^2-n^2}}, \quad \alpha_2 = \frac{(1-N)}{n}\sqrt{\frac{4n^2-1}{N^2-n^2}}, \quad \alpha_3 = \frac{(n-1)}{n}\sqrt{\frac{2n+1}{2n-3}}\sqrt{\frac{N^2-(n-1)^2}{N^2-n^2}}$$

The starting values for the above recursion are obtained from the equations as follows: $t_0(x) = \frac{1}{\sqrt{N}}$, $t_1(x) = (2x+1-N)\sqrt{\frac{3}{N(N^2-1)}}$,

The recurrence relation to compute the polynomials $t_n(x)$ is given as follows:

$$t_n(0) = \sqrt{\frac{N-n}{N+n}}\sqrt{\frac{2n+1}{2n-1}}t_{n-1}(0),$$

$$t_n(1) = \left\{1 + \frac{n(1+n)}{1-N}\right\}t_n(0),$$

$$t_n(x) = \gamma_1 t_n(x-1) + \gamma_2 t_n(x-2),$$

For n=1, 2, ..., N-1 and x=2, 3, ..., $\left(\frac{N}{2}-1\right)$, where

$$\gamma_1 = \frac{-n(n+1)-(2x-1)(x-N-1)-x}{x(N-x)}, \quad \gamma_2 = \frac{(x+1)(x-N-1)}{x(N-x)},$$

The above definition uses following scale factor for the polynomial of degree n:

$$\beta(n,N) = \sqrt{\frac{N(N^2-1)(N^2-2^2)...(N^2-n^2)}{2n+1}}$$

The set $\{t_n(x)\}$ has a squared-norm given by $\rho(n,N) = \sum_{i=0}^{N-1}\{t_n(i)\}^2 = 1.0$

The description of squared-norm $\rho(\cdot)$ and the properties of orthonormal Tchebichef polynomials are explained by Mukundan [12]. The first four discrete orthonormal Tchebichef moments are shown in Figure 1.

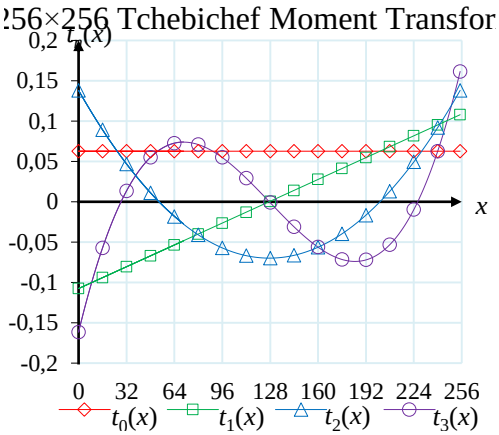

Figure 1. The first four discrete 256×256 Tchebichef polynomials $t_n(x)$ for x=0, 1, 2 and 3

The inverse TMT image reconstruction from its moments is given as follows:

$$\tilde{f}(x,y) = \sum_{m=0}^{M-1}\sum_{n=0}^{N-1} k_m(x) T_{mn} k_n(y)$$

For m, n = 0, 1, 2, ..., N-1. Where $\tilde{f}(x,y)$ denotes the reconstructed intensity distribution and M, N denote the maximum order of moments being used.

3 Experimental Designs

In this quantitative experiment, 80 images (24-bit RGB with 512×512 pixels) [13] are chosen to be tested and analyzed in order to develop psychovisual threshold in image compression. In past project work, psychovisual threshold has been investigated on 8×8 discrete transform [14-16]. First, the sample RGB image is converted into YCbCr colour space. An image is divided into the 256×256 block of image pixels. Each block of the image pixels is transformed by a two-dimensional 256×256 TMT. Based on the discrete orthonormal Tchebichef moments above, a compact representation of the moment coefficient $K_{(S\times S)}$ is given as follows:

$$K_{S\times S} = \begin{bmatrix} k_0(0) & k_1(0) & \cdots & k_{S-1}(0) \\ k_0(1) & k_1(1) & \cdots & k_{S-1}(1) \\ k_0(2) & k_1(2) & \cdots & k_{S-1}(2) \\ \vdots & \vdots & \ddots & \vdots \\ k_0(S-1) & k_1(S-1) & \cdots & k_{S-1}(S-1) \end{bmatrix}$$

The image block matrix by $F_{(256\times256)}$ with $f(x, y)$ denotes the intensity value of the image pixels on each colour component:

$$F_{S\times S} = \begin{bmatrix} f(0,0) & f(0,1) & \cdots & f(0,S-1) \\ f(1,0) & f(1,1) & \cdots & f(1,S-1) \\ f(2,0) & f(2,1) & \cdots & f(2,S-1) \\ \vdots & \vdots & \ddots & \vdots \\ f(S-1,0) & f(S-1,1) & \cdots & f(S-1,S-1) \end{bmatrix}$$

The matrix $T_{(S\times S)}$ of moments is defined using matrix size S=256 above as follows:

$$T_{(256\times256)} = K^T_{(256\times256)} F_{(256\times256)} K_{(256\times256)}$$

This process is repeated for every block in the original image to generate TMT frequency coefficient. The inverse moment relation of the reconstructed block image from the above moments is given as follows:

$$G_{(256\times256)} = K_{(256\times256)} T_{(256\times256)} K^T_{(256\times256)}$$

where $G_{(256\times256)}$ denotes the matrix image of the reconstructed intensity value. In this quantitative experiment, the contribution of each 256×256 TMT coefficient is investigated by incrementing it on each frequency order. The effect of incrementing TMT coefficient is measured by the reconstruction error per pixel.

The average reconstruction error is set as a smooth curve for a given frequency order zero to the maximum frequency order 510. An ideal smooth curve of average reconstruction error has been set as the psychovisual threshold. The ideal smooth curve is designed to give an optimal balance between the quality of the image output and the compression rate. The ideal average reconstruction error of incrementing 256×256 TMT coefficients for luminance and chrominance is shown in Figure 2. The ideal curve of average reconstruction error for a given frequency order 0 to frequency order 510 for luminance channel is visualized by a red curve, whereas for chrominance channel is depicted by a blue curve.

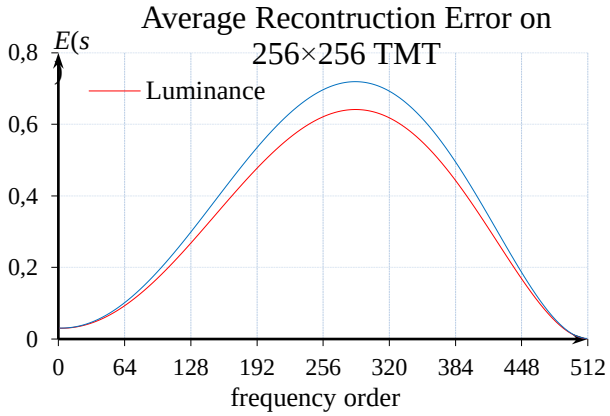

Figure 2. Average reconstruction error of incrementing TMT coefficients on 256×256 TMT luminance and chrominance for 40 real images

The x-axis represents frequency order and y-axis represents average reconstruction error. These curves are then interpolated by polynomial functions for luminance f_{ML} and chrominance f_{MR} as follows:

$$f_{ML}(x) = 0.000000000000305848x^5 - 0.00000000024827x^4 + 0.000000014256x^3 + 0.00001672x^2 - 0.0000506x + 0.0303$$

$$f_{MR}(x) = 0.000000000000034721x^5 - 0.0000000002815x^4 + 0.0000000162x^3 + 0.0000189x^2 - 0.0000576x + 0.0303$$

for a given frequency order x = 0, 1, 2, ..., 510. Further, these psychovisual thresholds are used to generate finer 256×256 TMT quantization values on each frequency order. Due to the large size of their new 256×256 quantization values, it is not possible to present the whole quantization matrix within a limited space in this paper. Therefore, the indexes 256×256 quantization values are presented by traversing the quantization table on each frequency order in a zigzag pattern as shown in Table 1. The finer 256×256 TMT quantization values for luminance and chrominance channels on each frequency order are shown in Table 2 and Table 3 respectively. The finer 256×256 TMT quantization tables are listed as a traversing array in a zigzag pattern. A large 256×256 quantization table consists of frequency order zero to the maximum of frequency order 510.

Table 1. The index of quantization values for each frequency order

0	1	5	6	14	15	27	28	44	45	65	66	90	91	119	120	152	153	189	190	230	231	275
2	4	7	13	16	26	29	43	46	64	67	89	92	118	121	151	154	188	191	229	232	274	276
3	8	12	17	25	30	42	47	63	68	88	93	117	122	150	155	187	192	228	233	273	277	318
9	11	18	24	31	41	48	62	69	87	94	116	123	149	156	186	193	227	234	272	278	317	319
10	19	23	32	40	49	61	70	86	95	115	124	148	157	185	194	226	235	271	279	316	320	357
20	22	33	39	50	60	71	85	96	114	125	147	158	184	195	225	236	270	280	315	321	356	358
21	34	38	51	59	72	84	97	113	126	146	159	183	196	224	237	269	281	314	322	355	359	392
35	37	52	58	73	83	98	112	127	145	160	182	197	223	238	268	282	313	323	354	360	391	393
36	53	57	74	82	99	111	128	144	161	181	198	222	239	267	283	312	324	353	361	390	394	423
54	56	75	81	100	110	129	143	162	180	199	221	240	266	284	311	325	352	362	389	395	422	424
55	76	80	101	109	130	142	163	179	200	220	241	265	285	310	326	351	363	388	396	421	425	450
77	79	102	108	131	141	164	178	201	219	242	264	286	309	327	350	364	387	397	420	426	449	451
78	103	107	132	140	165	177	202	218	243	263	287	308	328	349	365	386	398	419	427	448	452	473
104	106	133	139	166	176	203	217	244	262	288	307	329	348	366	385	399	418	428	447	453	472	474
105	134	138	167	175	204	216	245	261	289	306	330	347	367	384	400	417	429	446	454	471	475	492
135	137	168	174	205	215	246	260	290	305	331	346	368	383	401	416	430	445	455	470	476	491	493
136	169	173	206	214	247	259	291	304	332	345	369	382	402	415	431	444	456	469	477	490	494	507
170	172	207	213	248	258	292	303	333	344	370	381	403	414	432	443	457	468	478	489	495	506	508
171	208	212	249	257	293	302	334	343	371	380	404	413	433	442	458	467	479	488	496	505	509	
209	211	250	256	294	301	335	342	372	379	405	412	434	441	459	466	480	487	497	504	510		
210	251	255	295	300	336	341	373	378	406	411	435	440	460	465	481	486	498	503				
252	254	296	299	337	340	374	377	407	410	436	439	461	464	482	485	499	502					
253	297	298	338	339	375	376	408	409	437	438	462	463	483	484	500	501						

Table 2. The TMT quantization values for each frequency order on luminance

8	7	5	5	4	4	4	4	6	6	9	9	12	12	16	16	19	19	20	20	19	19	18
6	5	5	4	4	4	5	6	6	8	9	12	12	16	16	19	19	20	20	19	19	18	19
5	4	4	4	4	5	6	6	8	9	12	13	15	16	18	19	20	20	19	19	18	19	20
4	4	4	4	5	6	6	8	9	12	13	15	16	18	19	20	20	19	19	18	19	20	21
4	4	4	5	5	6	8	9	12	13	15	16	18	19	20	20	19	19	18	19	20	21	21
4	4	5	5	7	8	9	11	13	15	16	18	19	20	20	19	19	18	19	20	21	21	21
4	5	5	7	8	9	11	13	15	16	18	19	20	20	19	19	18	19	20	21	21	21	20
5	5	7	8	10	11	13	15	17	18	19	20	20	19	19	18	19	20	21	21	21	20	20
5	7	7	10	11	13	15	17	18	19	20	20	19	19	18	19	20	21	21	21	20	20	17
7	7	10	11	13	15	17	18	19	20	20	20	18	18	19	20	21	21	21	20	20	17	17
7	10	11	14	15	17	18	19	20	20	20	18	18	19	20	21	21	21	20	19	17	17	13
10	11	14	14	17	18	19	20	20	20	18	18	19	20	21	21	21	20	19	17	17	14	13
10	14	14	17	18	19	20	20	20	18	18	19	20	21	21	21	20	19	17	17	14	13	9
14	14	17	18	19	20	20	20	18	18	19	20	21	21	21	20	19	18	16	14	13	9	9
14	17	18	19	20	20	20	18	18	19	20	21	21	21	20	19	18	16	14	13	10	9	5
17	17	20	20	20	20	18	17	19	20	21	21	21	20	19	18	16	14	13	10	8	5	5
17	20	20	20	20	18	17	19	20	21	21	21	20	19	18	16	14	12	10	8	5	4	2
19	20	20	20	18	17	19	20	21	21	21	20	19	18	16	14	12	10	8	6	4	2	2
20	20	20	18	17	19	20	21	21	21	20	19	18	16	15	12	10	8	6	4	2	2	
20	20	18	17	19	20	21	21	21	20	19	18	16	15	12	11	8	6	4	2	2		
20	18	17	20	20	21	21	21	20	19	18	16	15	12	11	7	6	3	2				
17	17	20	20	21	21	21	20	19	18	15	15	11	11	7	6	3	3					
17	20	20	21	21	20	20	19	18	15	15	11	11	7	7	3	3						

Table 3. The TMT quantization values for each frequency order on chrominance

8	7	5	5	4	4	5	5	6	7	9	10	14	14	18	18	21	21	23	23	22	21	21
6	5	5	4	4	5	5	6	7	9	10	13	14	18	18	21	21	23	23	22	21	21	21
5	4	4	4	5	5	6	7	9	10	13	14	18	18	21	21	23	23	22	21	21	21	23
4	4	4	4	5	6	7	9	10	13	14	17	18	21	21	23	23	22	21	21	21	23	23
4	4	4	5	6	7	9	10	13	14	17	18	21	21	23	23	22	21	21	21	23	23	23
4	4	5	6	7	9	10	13	15	17	19	21	21	22	23	22	21	20	21	23	23	23	23
4	5	6	7	9	11	13	15	17	19	21	22	22	23	22	21	20	21	23	23	23	23	22
5	6	7	8	11	12	15	17	19	21	22	22	23	22	21	20	21	23	23	23	23	22	22
5	8	8	11	12	15	17	19	20	22	22	23	22	21	20	21	23	23	23	23	22	22	19
8	8	11	12	15	17	19	20	22	22	23	22	21	20	21	23	23	23	23	22	22	19	19
8	11	12	15	16	19	20	22	22	23	22	21	20	21	23	23	23	23	22	21	19	18	14
11	12	15	16	19	20	22	22	23	22	21	20	21	23	23	23	23	22	21	19	18	15	14
12	16	16	19	20	22	22	23	22	21	20	22	23	23	23	23	22	21	19	18	15	14	9
16	16	19	20	22	22	23	22	21	20	22	23	23	23	23	22	21	19	18	15	14	10	9
16	20	20	22	22	23	22	20	20	22	23	23	23	23	22	21	19	18	15	14	10	9	5
20	20	22	22	22	22	20	20	22	22	23	23	23	22	21	20	18	15	13	10	9	5	4
20	22	22	22	22	20	20	22	22	23	23	23	22	21	20	18	15	13	10	8	5	4	2
22	22	22	22	20	19	22	22	23	23	23	22	21	20	17	16	13	11	8	5	4	2	2
22	22	22	20	20	22	22	23	23	23	23	21	20	17	16	13	11	8	6	4	2	2	
22	22	20	19	22	22	23	23	23	23	21	20	17	16	13	11	8	6	3	2	2		
22	20	19	22	22	23	23	23	23	21	20	17	16	12	11	7	6	3	2				
20	19	22	22	23	23	23	23	21	20	17	16	12	12	7	6	3	2					
20	22	22	23	23	23	23	20	20	17	16	12	12	7	7	3	2						

There are $2^{16} = 65536$ quantization values from a 256×256 quantization table. The order 0 resides in the top left most corner of the quantization matrix order of $Q(0,0)$. The first order represents the quantization values of $Q(1,0)$ and $Q(0,1)$. The second order represents $Q(2,0)$, $Q(1,1)$ and $Q(0,2)$. For each frequency order, the same quantization value is assigned to them. The finer 256×256 TMT quantization values for a given frequency order 0 to frequency order 510 are visualized in Figure 3.

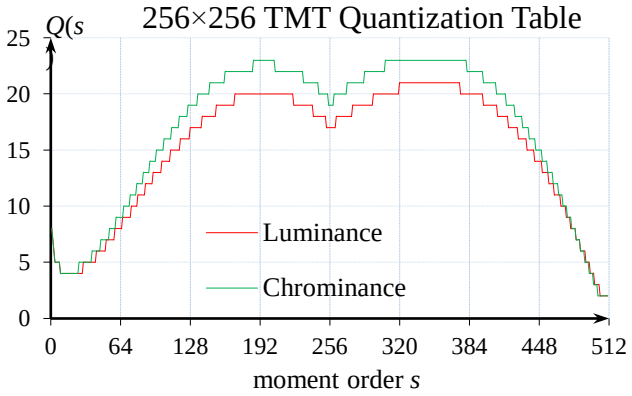

Figure 3. The finer 256×256 TMT quantization tables for luminance and chrominance for image compression

The smoother 256×256 TMT quantization table on the luminance channel is designed to take smaller values than chrominance channel. The investigation results show the contribution of the TMT coefficients to the reconstruction error is mainly concentrated on the middle frequency order. The effect of incrementing TMT coefficients on the middle frequency order gives a significant reconstruction error. According to Figure 3, there are two hills in the 256×256 TMT quantization tables. The impact of incrementing TMT coefficients on the middle frequency order produces a higher average reconstruction error than other frequency orders. In addition, the contribution of the TMT coefficients on the middle frequency order provides less effect to the compression rate. Therefore, the finer 256×256 TMT quantization tables from the psychovisual threshold on the middle frequency order are designed to generate lower quantization values.

4 Experimental Results

The smoother 256×256 TMT quantization tables from the psychovisual threshold are tested in image compression. The 80 images are evaluated in image compression. The 80 images are classified into 40 real images and 40 graphical images.

Table 4. Average Bit Length of Huffman Code on the Output Compressed Image from 40 Real Images and 40 Graphical Images

Method	Real Images			Graphical Images		
	ACY	ACCr	ACCb	ACY	ACCr	ACCb
8×8 JPEG Quantization Tables	2.868	2.095	2.184	2.965	2.505	2.515
8×8 TMT Quantization Tables	1.767	1.212	1.260	2.040	1.983	2.061
8×8 TMT Psychovisual Threshold	1.764	1.166	1.191	2.027	1.625	1.745
256×256 TMT Psychovisual Threshold	2.095	1.218	1.251	2.279	1.521	1.637

Table 5. An Image Quality Measurement on the Output Compressed Image from 40 Real Images and 40 Graphical Images

Method	Real Images			Graphical Images		
	Full Error	PSNR	SSIM	Full Error	PSNR	SSIM
8×8 JPEG Quantization Tables	5.535	31.190	0.956	5.648	31.636	0.957
8×8 TMT Quantization Tables	5.258	31.372	0.947	4.840	32.274	0.952
8×8 TMT Psychovisual Threshold	5.246	31.379	0.946	4.767	32.363	0.951
256×256 TMT Psychovisual Threshold	4.671	32.572	0.948	4.280	33.704	0.949

The performance of the large TMT quantization tables from the TMT psychovisual threshold is measured by average bit length of Huffman code and image quality measurement. The average bit length of Huffman code and the average image reconstruction error from the proposed finer 256×256 TMT quantization tables are shown in Table 4 and Table 5 respectively. A sample Baboon image is selected from 80 images [13] in order to analyse the visual quality of the compressed image. The right eye of the Baboon image is chosen and analysed perceptually on the rich pattern of image pixels. The visual outputs of JPEG image compression, 8×8 TMT psychovisual threshold and the proposed 256×256 TMT psychovisual threshold are projected in Figure 4. The image compression using default JPEG quantization tables through 8×8 DCT produces artifact images and blur in image output when the visual output is zoomed in to 400% as shown in Figure 4(b). The optimal 8×8 TMT quantization tables from the psychovisual threshold give a slightly better visual quality on the compressed image as depicted in Figure 4(c) than the standard JPEG image compression. However, the visual image output is still a little bit blur and carries blocking effect along the boundaries. While, the psychovisual thresholds on large TMT image compression produces largely free of the blocking artifact as shown in Figure 4(d).

(a) (b) (c) (d)

Figure 4. Original right eye of Baboon image (a), 8×8 JPEG compression (b), 8×8 TMT psychovisual threshold (c) and 256×256 TMT psychovisual threshold (d) zoomed in to 400%.

In addition, the finer 256×256 TMT quantization tables from the psychovisual threshold produce the richer texture of the Baboon right eye. The image compression using psychovisual threshold on large TMT produces significantly better visual quality on the output image than standard JPEG image compression. A visual inspection on the sample output image from the finer 256×256 TMT quantization tables points out the fact that it produces almost the same texture image pixels of the original Baboon image as shown in the blue circle.

5 Conclusions

The psychovisual threshold provides a significant impact on image compression. This research has designed the psychovisual threshold on large Tchebichef

moments for image compression. The psychovisual threshold is practically the best measure on an optimal amount of frequency image signals to be lossy encoded. This quantitative experiment shows the critical role of psychovisual threshold as a basic primitive to generate quantization table in image compression. The finer large Tchebichef quantization tables can then be generated from the psychovisual threshold. The psychovisual threshold on large Tchebichef moment has made significant improvement in the Tchebichef image compression performance. The smoother large Tchebichef quantization tables from the psychovisual threshold produce better visual quality of the output image and smaller average bit length of Huffman code than standard JPEG image compression. At the same time, the psychovisual threshold on large Tchebichef moments manages to overcome the blocking effect which often occurs in standard JPEG image compression. This psychovisual threshold is designed to support practical image compression for high fidelity digital images in the near future.

Acknowledgements. The authors would like to express a very special thanks to Ministry of Education, Malaysia for providing financial support by Fundamental Research Grant Scheme (FRGS/2012/FTMK/SG05/03/1/F00141).

References

[1] S. Lee and S.J. Park, A new image quality assessment method to detect and measure strength of blocking artifacts, Signal Processing: Image Communication, 27 (1) (2012), 031-038.

[2] J. Singh, S. Singh, D. Singh and M. Uddin, Detection method and filters for blocking effect reduction of highly compressed images, Signal Processing: Image Communication, 26 (8) (2011), 493-506.

[3] J. Singh, S. Singh, D. Singh and M. Uddin, A signal adaptive filter for blocking effect reduction of JPEG compressed images, International Journal of Electronics and Communications, 65 (10) (2011), 827– 839.

[4] F. Ernawan, N.A. Abu and N. Suryana, An optimal Tchebichef moment quantization using psychovisual threshold for image compression, Advanced Science Letters, 20 (1) (2014), 070-074.

[5] N.A. Abu, F. Ernawan, N. Suryana and S. Sahib, Image watermarking using psychovisual threshold over the edge, Information and Communication Technology, 7804 (2013), 519-527.

[6] F. Ernawan, N.A. Abu and N. Suryana, TMT quantization table generation based on psychovisual threshold for image compression, International Conference of Information and Communication Technology (ICoICT 2013), (2013), 202-207.

[7] N.A. Abu, F. Ernawan and S. Sahib, Psychovisual model on discrete orthonormal transform, International Conference on Mathematical Sciences and Statistics (ICMSS 2013), (2013), 309-314.
[8] F. Ernawan, N.A. Abu and N. Suryana, A psychovisual threshold for generating quantization process in Tchebichef moment image compression, Journal of Computers, 9 (3) (2014), 702-710.
[9] F. Ernawan, N.A. Abu and N. Suryana, Adaptive Tchebichef moment transform image compression using psychovisual model, Journal of Computer Science, 9 (6) (2013), 716-725.
[10] F. Ernawan, E. Noersasongko and N.A. Abu, An efficient 2×2 Tchebichef moments for mobile image compression, International Symposium on Intelligent Signal Processing and Communication System (ISPACS 2011), (2011), 001-005.
[11] N.A. Abu, F. Ernawan and N. Suryana, An image dithering via Tchebichef moment transform, Journal of Computer Science, 9 (7) (2013), 811-820.
[12] R. Mukundan, Some computational aspects of discrete orthonormal moments, IEEE Transactions on Image Processing, 13 (8) (2004), 1055-1059.
[13] R. Rodriguez-Sanchez, J. Martinez-Baena, A. Garrido, J.A. Garcia, J. Fdez-Valdivia, M.C. Aranda, Computer Vision Group, University of Granada, [Online], (2002), Available: http://decsai.ugr.es/cvg/dbimagenes/c512.php.
[14] N.A. Abu, F. Ernawan and N. Suryana, A generic psychovisual error threshold for the quantization table generation on JPEG image compression, 9th International Colloquium on Signal Processing and its Applications, (2013), 039-043.
[15] F. Ernawan, N.A. Abu and N. Suryana, An adaptive JPEG image compression using psychovisual model, Advanced Science Letters, 20 (1) (2014), 026-031.
[16] F. Ernawan, N.A. Abu and N. Suryana, Integrating a smooth psychovisual threshold into an adaptive JPEG image compression, Journal of Computers, 9 (3) (2014), 644-653.

Received: August 11, 2014